Astronomy: A Physical Perspective

Marc L. Kutner

CAMBRIDGE
UNIVERSITY PRESS

PUBLISHED BY THE PRESS SYNDICATE OF THE UNIVERSITY OF CAMBRIDGE
The Pitt Building, Trumpington Street, Cambridge, United Kingdom

CAMBRIDGE UNIVERSITY PRESS
The Edinburgh Building, Cambridge CB2 2RU, UK
40 West 20th Street, New York, NY 10011-4211, USA
477 Williamstown Road, Port Melbourne, VIC 3207, Australia
Ruiz de Alarcón 13, 28014 Madrid, Spain
Dock House, The Waterfront, Cape Town 8001, South Africa

http://www.cambridge.org

First edition published by John Wiley & Sons, 1987

Printed in the United Kingdom at the University Press, Cambridge

Typeface Swift-Regular 9.5/12.25 *System* QuarkXpress [TB]

A catalog record for this book is available from the British Library

Library of Congress Cataloging in Publication data

Kutner, Marc Leslie.
Astronomy: a physical perspective / Marc Kutner.
p. cm.
Includes bibliographical references and index.
ISBN 0 521 82196 7–ISBN 0 521 52927 1 (pb.)
1. Astronomy. I. Title.

QB45.2 .K87 2003
520–dc21 2002034946

ISBN 0 521 82196 7 hardback
ISBN 0 521 52927 1 paperback

Contents

Chapter 6

The Sun: a typical star

The Sun (Fig. 6.1) is the only star we can study in any detail. It therefore serves as a guide to our pictures of other stars. Any theory of stellar structure must first be able to explain the Sun before explaining other stars. As we have seen, the Sun's spectral type places it in the mid-range of main sequence stars. If we understand the Sun, we have the hope of being able to understand a significant number of other types of stars.

6.1 Basic structure

We have already seen that the mass of the Sun is 2.0×10^{33} g and that its radius is 7×10^{10} cm (7×10^5 km). Its average density is

$$\rho = \frac{M_\odot}{(4\pi/3)R_\odot^3}$$

$$= \frac{2 \times 10^{33}\,\mathrm{g}}{(4\pi/3)(7 \times 10^{10}\,\mathrm{cm})^3}$$

$$= 1.4\ \mathrm{g/cm^3}$$

For comparison, the density of water is 1 g/cm^3. The Sun is composed mostly of hydrogen (94% by the number of atoms), with some helium (6% by number of atoms), and only 0.1% other elements. The abundances of the elements are given in Appendix G. Our best measurement of the effective temperature of the Sun is 5762 K. The solar luminosity is 3.8×10^{33} erg/s. (The effective temperature is the temperature that we use in the Stefan–Boltzmann law to give the solar luminosity.)

When we look at the Sun, we see only the outermost layers. We have to deduce the internal structure from theories of stellar structure (which we will discuss in Chapter 9). The basic structure of the Sun is shown in Fig. 6.2. The center is the *core*. It is the source of the Sun's energy. Its radius is about 10% of the full solar radius. The outermost layers form the atmosphere. We divide the atmosphere into three parts. Most of the light we see comes from the *photosphere*, the bottom layer of the atmosphere. Above the photosphere is the *chromosphere*, named because it is the source of red light seen briefly during total eclipses of the Sun. The chromosphere is about 10^4 km thick. The outermost layer is the *corona*, which extends far into space. It is very faint, and, for most of us, can only be seen during total solar eclipses. Beyond the corona, we have the *solar wind*, not strictly part of the Sun, but a stream of particles from the Sun into interplanetary space.

6.2 Elements of radiation transport theory

Radiation is being emitted and absorbed in the Sun in all layers. However, we see radiation mostly from the surface. Most radiation from below is absorbed before it reaches the surface. To understand what we are seeing when we look at the Sun, we need to understand about the interaction between radiation and matter. For example, much of what we know about the solar atmosphere comes from studying spectral lines as well as the continuum. In studying how radiation interacts with matter, known as *radiation transport theory*, we see how to use spectral lines

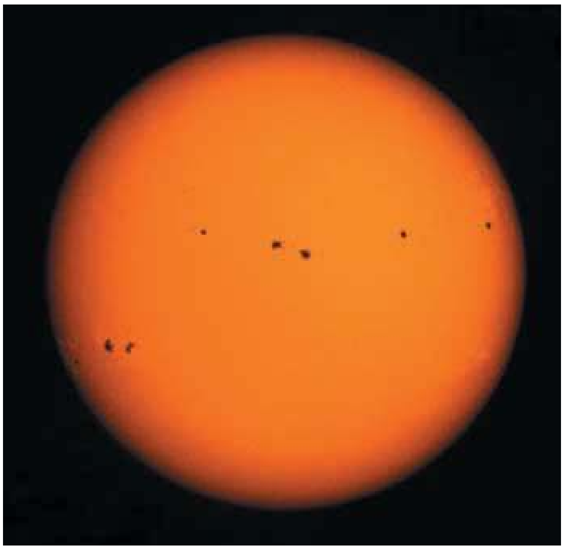

Fig 6.1. The Sun. [NOAO/AURA/NSF]

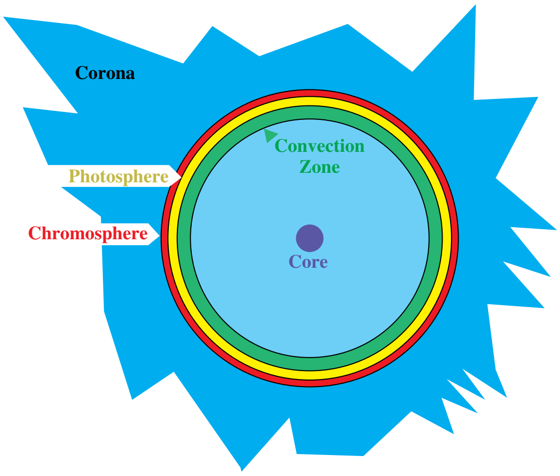

Fig 6.2. Basic structure of the Sun.

to extract detailed information about the solar atmosphere.

We first look at the absorption of radiation by atoms in matter. We can think of the atoms as acting like small spheres, each of radius r (Fig. 6.3). Each sphere absorbs any radiation that strikes it. To any beam of radiation, a sphere looks like a circle of projected area πr^2. If the beam is within that circle, it will strike the sphere and be absorbed. We say that the *cross section* for striking a sphere is $\sigma = \pi r^2$. The concept of a cross section carries over into quantum mechanics. Instead of the actual size of an atom, we use the effective area over which some process (such as absorption) takes place. So then r would be how close the photon would have to be to the atom in order to be absorbed.

We consider a cylinder of these spheres, with the radiation entering the cylinder from one end. We would like to know how much radiation is absorbed, and how much passes through to the far end. We let n be the number of spheres per unit volume. The cylinder has length l and area A, so the volume is Al. The number of spheres in the cylinder is

$$N = n\,Al \tag{6.1}$$

We define the total cross section of all the spheres as the number of spheres multiplied by the cross section per sphere:

$$\sigma_{\rm tot} = N\,\sigma \tag{6.2}$$

$$\sigma_{\rm tot} = n\,A\,l\,\sigma \tag{6.3}$$

In making this definition, we have assumed that the incoming beam can "see" all the spheres. No sphere blocks or shadows another. We are assured of little shadowing if the spheres occupy a small fraction of the area, as viewed from the end. That is

$$\sigma_{\rm (tot)} \ll A \tag{6.4}$$

Under these conditions, the fraction of the incoming radiation that will be absorbed, f, is just that fraction of the total area A that is covered by the spheres. That is

$$f = \sigma_{\rm (tot)}/A \tag{6.5}$$

Using equation (6.3), this becomes

$$f = n\sigma\,l \tag{6.6}$$

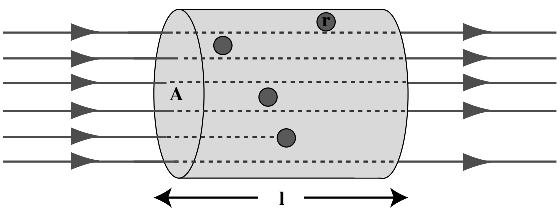

Fig 6.3. Absorption of radiation. Radiation enters from the left. Any beam striking a sphere is absorbed.

We define the *optical depth* to be this quantity:

$$\tau = n\sigma l \tag{6.7}$$

Our requirement in equation (6.4) reduces to $\tau \ll 1$. Under this restriction, the optical depth of any section of material is simply the fraction of incoming radiation that is absorbed when the radiation passes through that material. (For example, if the optical depth is 0.01, then 1% of the incoming radiation is absorbed.)

In general, σ will be a function of wavelength. For example, we know that at a wavelength corresponding to a spectral line, a particular atom will have a very large cross section for absorption. At a wavelength not corresponding to a spectral line, the cross section will be very small. To remind us that σ is a function of λ (or ν), we write it as σ_λ (or σ_ν). This means that the optical depth is also a function of λ (or ν), so we rewrite equation (6.7) as

$$\tau_\lambda = nl\sigma_\lambda \tag{6.8}$$

In our discussions, the quantity nl occurs often. It is the product of a number density and a length, so its units are measured in number per unit area. It is the number of particles along the full length, l, of the cylinder per unit surface area. For example, if we are measuring lengths in centimeters, it is the number of particles in a column whose face surface area is 1 cm^2, and whose length is l, the full length of the cylinder. We call this quantity the *column density*.

We can see that the optical depth depends on the properties of the material – e.g. cross section and density of particles – and on the overall size of the absorbing region. It is sometimes convenient to separate these two dependencies by defining the *absorption coefficient*, which is the optical depth per unit length through the material,

$$\kappa_\lambda = \frac{\tau_\lambda}{l} \tag{6.9a}$$

$$= n\sigma_\lambda \tag{6.9b}$$

If κ_λ gives the number of absorptions per unit length, then its inverse gives the mean distance between absorptions. This quantity is called the *mean free path*, and is given by

$$L_\lambda = 1/\kappa_\lambda \tag{6.10}$$

$$= 1/n\sigma_\lambda \tag{6.11}$$

In terms of these quantities, the optical depth is given by

$$\tau_\lambda = \frac{l}{L_\lambda} \tag{6.12a}$$

$$= \kappa_\lambda l \tag{6.12b}$$

In the above discussion, we required that the optical depth be much less than unity. Our interpretation of τ as the fraction of radiation absorbed only holds for $\tau \ll 1$. What if that is not the case? We then have to divide our cylinder into several layers. If we make the layers thin enough, we can be assured that the optical depth for each layer will be very small. We then follow the radiation through, layer by layer, looking at the fraction absorbed in each layer (Fig. 6.4).

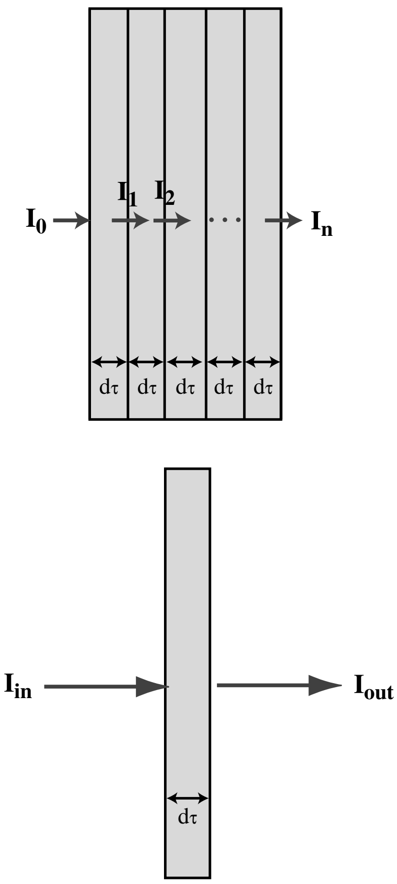

Fig 6.4. Radiation passing through several layers. Each layer has an optical depth dτ. The bottom of the figure is for calculating the effect of each layer.

Let's look at the radiation passing through some layer with optical depth $d\tau$. Since $d\tau \ll 1$, it is the fraction of this radiation that is absorbed. The amount of radiation absorbed in this layer is $I\,d\tau$. The amount of radiation passing through to the next layer is $I(1 - d\tau)$. The change in intensity, dI, while passing through the layer, is

$$dI = I_{out} - I_{in} \quad (6.13)$$

$$= -I\,d\tau \quad (6.14)$$

Notice that dI is negative, since the intensity is decreased in passing through the layer.

Now that we know how to treat each layer, we must add up the effect of all the layers to find the effect on the whole sample of material. We can see that we have formulated the problem so that we are following I as a function of τ. We let τ' be the optical depth through which the radiation has passed by the time it reaches a particular layer, and I' be the intensity reaching that layer. Then τ' ranges from zero, at the point where the radiation enters the material, to τ, the full optical depth where the radiation leaves the material. Over that range, I' varies from I_0, the incident intensity, to I, the final intensity. Using equation (6.14),

$$dI'/I' = -d\tau' \quad (6.15)$$

In this form, all of the I' dependence is on the left, and the τ' dependence is on the right. To add up the effect of the layers, we integrate equation (6.15) between the limits given above:

$$\int_{I_0}^{I} \frac{dI'}{I} = -\int_0^{\tau} d\tau'$$

$$\ln(I) - \ln(I_0) = -\tau \quad (6.16)$$

Using the fact that $\ln(a/b) = \ln(a) - \ln(b)$, this becomes

$$\ln(I/I_0) = -\tau \quad (6.17)$$

Raising e to the value on each side, remembering that $e^{\ln x} = x$, and multiplying both sides by I_0 gives

$$I = I_0\,e^{-\tau} \quad (6.18)$$

We can check this result in the limit $\tau \ll 1$, called the *optically thin limit*, using the fact that

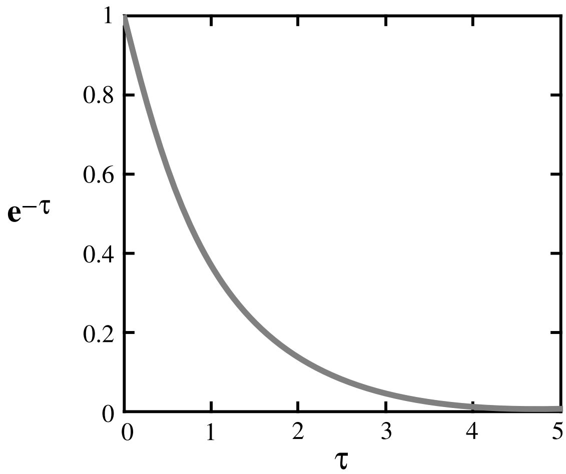

Fig 6.5. $e^{-\tau}$ vs. τ, showing the fall-off in transmitted radiation as the optical depth increases. Note that the curve looks almost linear for small τ. For large τ, it approaches zero asymptotically.

$e^x \cong 1 + x$, for $x \ll 1$. In this case, equation (6.18) becomes

$$I = I_0\,(1 - \tau) \quad (6.19)$$

This is the expected result for small optical depths, where τ again becomes the fraction of radiation absorbed.

As shown in Fig. 6.5, $e^{-\tau}$ falls off very quickly with τ. This means that to escape from the Sun, radiation must come from within approximately one optical depth of the surface. This explains why we only see the outermost layers. Since the absorption coefficient κ_λ is a function of wavelength, we can see to different depths at different wavelengths. At a wavelength where κ_λ is large, we don't see very far into the material. At wavelengths where κ_λ is small, it takes a lot of material to make $\tau_\lambda = 1$. We take advantage of this to study conditions at different depths below the surface.

So far we have only looked at the absorption of radiation passing through each layer. However, radiation can also be emitted in each layer, and the amount of emission also depends on the optical depth. In general, we must carry out complicated radiative transfer calculations to take all effects into account. To solve these problems, we use powerful computers to make mathematical models of stellar atmospheres. In these calculations, we input the distribution of temperature, density and composition and predict the spectrum that we will see, including emission and absorption lines. We vary the input parameters until we find models that produce predictions that agree with the observations. The results of these calculations are not unique, but they do give us a feel for what processes are important in stellar atmospheres. The more observational data we can predict with the models, the more confident we can be that the temperatures, densities and compositions we derive are close to the actual ones.

6.3 The photosphere

Most of the visible photons we receive from the Sun originate in the photosphere. One question you might ask is why we see continuum radiation at all. We have already seen how atoms can emit or absorb energy at particular wavelengths, producing spectral lines. However, we have not discussed the source of the emission and absorption of the continuum. It turns out that the continuum opacity in the Sun at optical wavelengths comes from the presence of H^- ions. An H^- ion is an H atom to which an extra electron has been added. As you might guess, this extra electron is held only very weakly to the atom. Very little energy is required to remove it again. H^- ions are present because there is so much hydrogen, and there are a large number of free electrons to collide with those atoms.

If we have an H^- ion and a photon (γ) strikes it, the photon can be absorbed, and the electron set free:

$$H^- + \gamma \rightarrow H + e^-$$

The H^- ion is a bound system. The final state has an H atom and a free electron. We call this process a *bound–free* process. In such a process, the wavelength of the incoming photon is not restricted, as long as the photon has enough energy to remove the electron. The electron in the final state can have any kinetic energy, so a continuous range of photon energies is possible. This process then provides most of the continuum opacity of the photosphere. The continuum emission results from the inverse process.

6.3.1 Appearance of the photosphere

We have said that the Sun is the one star that we can study in great detail. To do this, we try to observe the photosphere with the best resolution possible. When we observe the Sun, the light-gathering power of our telescope is not usually a problem. Therefore, we can try to spread the image out over as large an area as possible, making it easier to see detailed structure. We therefore want a telescope with a long focal length to give us a large image scale. The solar telescope shown in Fig. 6.6 provides this type of detailed picture.

Fig 6.6. Solar telescope on Kitt Peak (operated by NOAO). The telescope has a very long focal length, so that two can produce a large image and study the detailed appearance. Since the tube is so long, it is not reasonable to move it. Instead, the large mirror at the top (the objective) is moved to keep the sunlight directed down the tube. [NOAO/AURA/NSF]

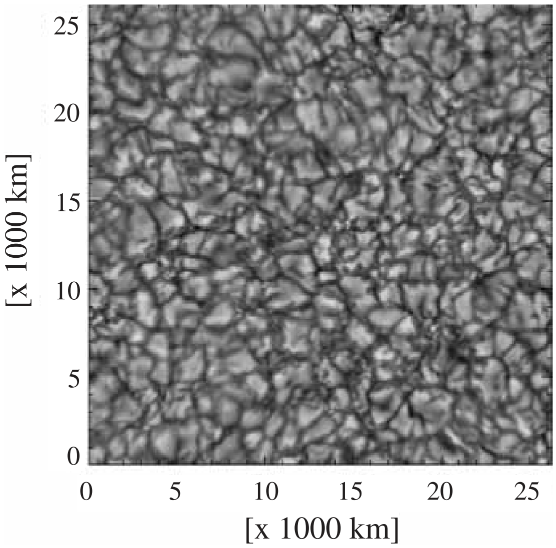

Fig 6.7. Granulation in the Sun. Remember, the darker areas are not really dark. They are only a little cooler than the bright areas. [NOAO/AURA/NSF]

When we look on a scale of a few arc seconds, we see that the surface of the Sun does not have a smooth appearance (Fig. 6.7). We see a structure, called *granulation*, in which lighter areas are surrounded by darker areas. The darker areas are not really dark. They are just a little cooler than the lighter areas, and only appear dark in comparison to the light areas. The granules are typically about 1000 km across. The pattern of granulation also changes with time, with a new pattern appearing every 5 to 10 min.

We interpret this granulation as telling us about the underlying structure we cannot see directly. The granulation can be explained by circulating cells of material, called *convection zones* (Fig. 6.8). (Convection is the form of energy transport in which matter actually moves from one place to another. Strong convection on the Earth is responsible for the updrafts that produce thunderstorms. A pot of boiling water also has energy transport by convection.) The brighter regions are warmer gas rising up from below. The dark regions are cooler gas falling back down.

In addition to the granulation variations, there is also a variation called the *five minute oscillation*, in which parts of the photosphere are moving up and down. We think this convection results

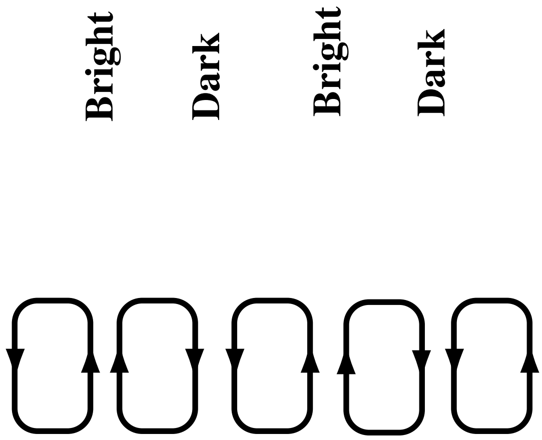

Fig 6.8. Granulation and convection zone. This is a side view to show what is happening below the surface. Hotter gas is being brought up from below, producing the bright regions. The cooler gas, which produces the darker regions, is carried down to replace the gas that was brought up.

from sound waves in the upper layers of the convection zone. This type of oscillation is one of many that are studied for clues to the Sun's interior structure. This area of research is called *solar seismology*. (On the Earth, seismologists study motions near the surface to learn about the interior.)

One interesting question about the photosphere concerns the sharpness of the solar limb. The Sun is a ball of gas whose density falls off continuously as one moves farther from the center. There is no sharp boundary (like the surface of the Earth), yet we see a definite edge on the Sun. In Fig. 6.9, we see some lines of sight through the

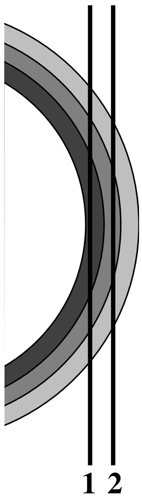

Fig 6.9. Lines of sight through the solar limb. For clarity, we think of the Sun as being composed of a series of spherical shells. The density in each shell decreases as we move farther from the center. This decreasing density is indicated by the shading; two lines of sight are indicated. Note that most of each line of sight is in the densest layer through which that particular line passes. Even though line 2 is not shifted very far from line 1, line 1 passes through much more material.

photosphere. As the line of sight passes farther from the center of the Sun, the opacity decreases because (1) the path length through the Sun is less, and (2) it passes through less dense regions. Since the amount of light getting through is proportional to $e^{-\tau}$, the effect of τ changing from line of sight to line of sight is enhanced by the exponential behavior. Therefore the transition from the Sun being mostly opaque to being mostly transparent takes place over a region that is small compared with our resolution, and the edge looks sharp.

6.3.2 Temperature distribution

Another interesting phenomenon near the solar limb can be seen in the photograph in Fig. 6.1. The Sun does not appear as bright near the limb as near the center. This *limb darkening* is also an optical depth effect, as shown in Fig. 6.10. We compare two lines of sight: (1) toward the center of the Sun from the observer, and (2) offset from the center of the Sun. In each line of sight, we can only see down to $\tau \cong 1$. Line of sight 1 is looking straight down into the atmosphere, so it gets closer to the center of the Sun before an optical depth of unity is reached than does line of sight 2, which has a longer path through any layer. We see deeper into the Sun on line of sight 1 than we do on line of sight 2. If the temperature decreases with increasing height in the photosphere, we are seeing hotter material on line of sight 1 than on 2, so line of sight 1 appears brighter than line of sight 2. Since line of sight 1 takes us the deepest into the Sun, we define the point at which τ reaches unity on this line as being the *base of the photosphere*. When we talk about the temperature of the Sun, we are talking about the temperature at the base of the photosphere.

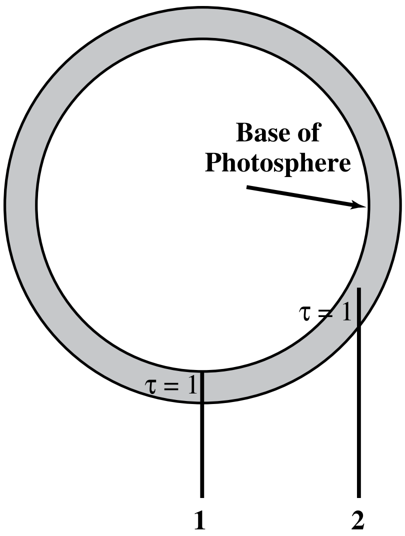

Fig 6.10. Limb darkening. Line of sight 1 is directed from the observer toward the center of the Sun, so it takes the shortest path through the atmosphere. This line allows us to see the deepest into the photosphere, and the base of the photosphere is defined to be where the optical depth τ along this line reaches unity. Line of sight 2 is closer to the edge, so it doesn't allow us to see as deep into the photosphere. If the temperature decreases with increasing height in the photosphere, then line of sight 1 allows us to see hotter material than does line of sight 2, and the edge of the Sun appears darker than the center.

When we look at the Sun, it appears brighter along line of sight 1 than it does along line of sight 2. This means that the Sun is hotter at the end of 1 than at the end of 2. From this, we conclude that the photosphere cools as one moves farther from the center of the Sun. If the photosphere became hotter as one moves farther from the center, we would see limb brightening.

We obtain more useful information about the photosphere by studying its spectral lines (Fig. 6.11). The spectrum shows a few strong absorption lines and a myriad of weaker ones. The stronger lines were labeled A through K by Fraunhofer in 1814. These lines have since been identified. For example, the C line is the first Balmer line (Hα); the D line is a pair of lines belonging to neutral sodium (NaI); and the H and K lines belong to singly ionized calcium (CaII). Sodium and calcium are much

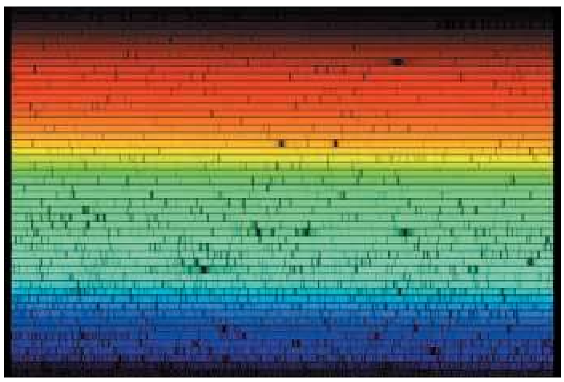

Fig 6.11. The solar spectrum. [NOAO/AURA/NSF]

less abundant than hydrogen but their absorption lines are as strong as Hα. We have already seen in Chapter 3 that this can result from the combined effects of excitation and ionization.

6.3.3 Doppler broadening of spectral lines

When we study the lines with good spectral resolution, we can look at the details of the line profile. The lines are broadened by Doppler shifts due to the random motions of the atoms and ions in the gas (Figs. 6.12 and 6.13). If all the atoms were at rest, all the photons from a given transition would emerge with a very small spread in wavelength. However, the atoms are moving with random speeds in random directions. We therefore see a spread in the Doppler shifts, and the line is broadened. This process is called *Doppler broadening*. If the gas is hotter, the spread in speeds is greater, and thus the Doppler broadening is also greater. If in addition to these random motions all the objects containing the particles have some overall motion that just shifts the center wavelength of the line, the broadening would still be the same.

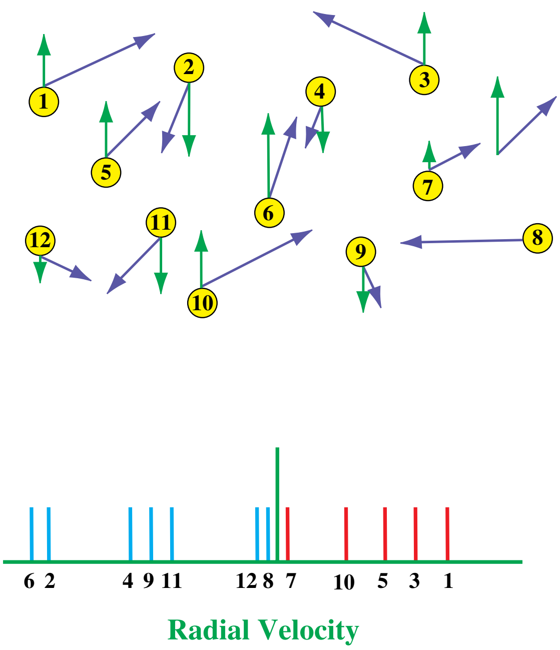

Fig 6.12. Doppler broadening. The top shows the (random) motions of a group of particles. The purple vectors are the actual velocities; the green vectors are the radial components, which produce the Doppler shift. For each particle, identified by a number, the radial velocities are plotted below. The line profile is the sum of all the individual Doppler shifted signals, and with many more particles it would have a smooth appearance.

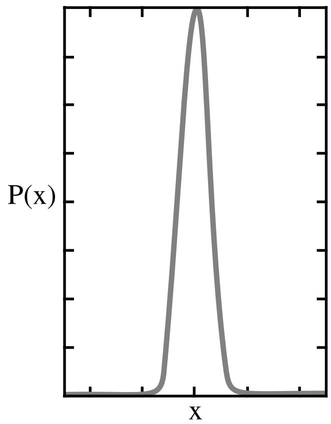

Fig 6.13. Line profile. We plot intensity as a function of wavelength.

We can estimate the broadening as a function of temperature. If $\langle v^2 \rangle$ is the average of the square of the random velocities in a gas, and m is the mass per particle, the average kinetic energy per particle is $(1/2)m\langle v^2 \rangle$. If we have an ideal monatomic gas, this should equal $(3/2)kT$, giving

$$(1/2)m\langle v^2 \rangle = (3/2)kT \tag{6.20}$$

Solving for $\langle v^2 \rangle$ gives

$$\langle v^2 \rangle = 3kT/m \tag{6.21}$$

Taking the square root gives the *root mean square (rms) speed*

$$v_{\mathrm{rms}} = \left(\frac{3kT}{m} \right)^{1/2} \tag{6.22}$$

This gives us an estimate of the range of speeds we will encounter. (The range will be larger, since we can have atoms coming toward us or away from us, and since some atoms will be moving faster than this average, but the radial velocity is reduced since only the component of motion along the line of sight contributes to the Doppler broadening.) To find the actual wavelength range over which the line is spread out, we would use the Doppler shift expression in equation (5.4).

Example 6.1 Doppler broadening

Estimate the wavelength broadening in the Hα line in a gas composed of hydrogen atoms at $T = 5500$ K.

SOLUTION
Using equation (6.22) gives

$$v_{\rm rms} = \left[\frac{(3)(1.38 \times 10^{-16}\ {\rm erg/K})(5.5 \times 10^3\ {\rm K})}{1.7 \times 10^{-24}\ {\rm g}}\right]^{1/2}$$

$$= 1.2 \times 10^6\ {\rm cm/s}$$

From equation (5.4), we estimate the linewidth as

$$\Delta\lambda = \lambda\left(\frac{v_{\rm rms}}{c}\right)$$

$$= \left(\frac{(656.28\ {\rm nm})(1.2 \times 10^6\ {\rm cm/s})}{(3 \times 10^{10}\ {\rm cm/s})}\right)^{1/2}$$

$$= 0.03\ {\rm nm}$$

In any spectral line, smaller Doppler shifts relative to the line center are more likely than larger ones. Therefore, the optical depth is greatest in the line center, and falls off to either side. At different Doppler shifts away from the line center, we will see different distances into the Sun. The farther we are from the line center, the deeper we see. By studying line profiles in detail we learn about physical conditions at different depths. Also, each spectral line has a different optical depth in the line center, so different lines allow us to see down to different depths in the photosphere. When we perform model stellar atmosphere calculations, we try to predict as many of the features of the spectrum as possible, including the relative strengths of various lines and the details of certain line profiles.

From observations of various spectral lines, the temperature profile for the photosphere has been derived. It is shown in Fig. 6.14. Note that the temperature falls as one goes up from the base of the photosphere. This is what we might expect, since we are moving farther from the heating source. However, an interesting phenomenon is observed. The temperature reaches a minimum at 500 km above the base of the photosphere, and then begins to rise with altitude. We will see below that this temperature rise continues into the higher layers.

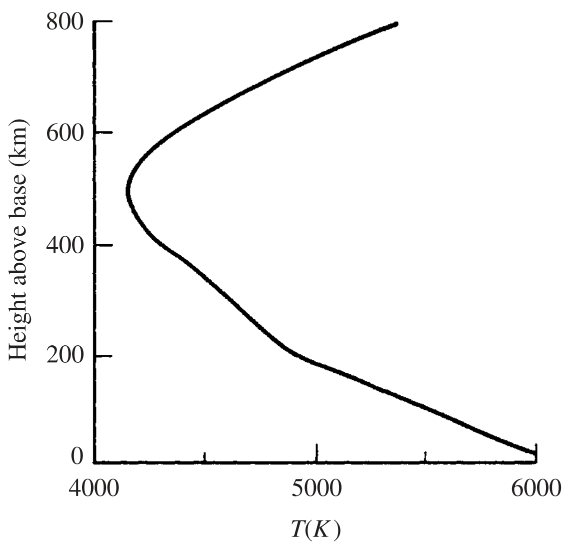

Fig 6.14. Temperature vs. height in the photosphere.

6.4 The chromosphere

At most wavelengths the chromosphere is optically thin, so we can see right through it to the photosphere. Under normal conditions the continuum radiation from the photosphere overwhelms that from the chromosphere. However, during a total eclipse of the Sun, just before and after totality, the Moon blocks the light from the photosphere, but not from the chromosphere. For that brief moment, we see the red glow of the chromosphere. The red glow comes from Hα emission. The optical depth of the Hα line is sufficiently large that we can study the chromosphere by studying that line. At the center of the Hα line we see down only to 1500 km above the base of the photosphere.

We can also study the large scale structure of the chromosphere by taking photographs through filters that only pass light from one line. One such photograph is shown in Fig. 6.15. In this picture we see granulation on an even larger scale than in the photosphere. This is called *supergranulation*. The supergranules are some 30 000 km across. As with the granules in the photosphere, the matter in the center of the supergranules is moving up and the matter at the edges is moving down. These motions can be determined from Doppler shifts of spectral lines. We also see smaller scale irregularities in the chromosphere, called *spicules*. These are protrusions from the surface some 700 km across and 7000 km high. An Hα image of the chromosphere is shown in Fig. 6.16.

When the chromosphere is visible just before and after totality, we see only a thin sliver of light.

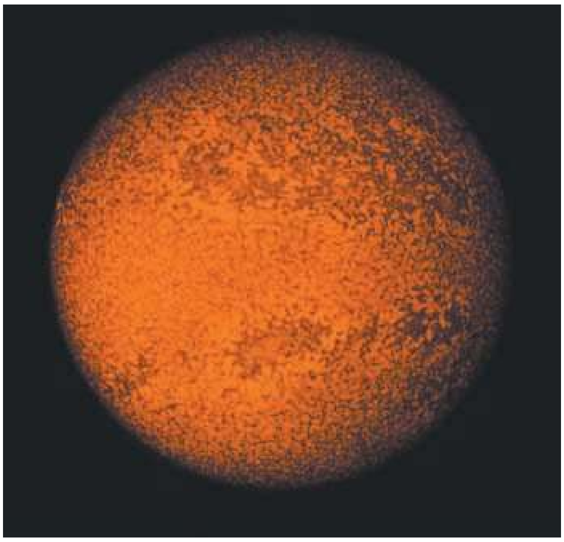

Fig 6.15. This spectroheliogram shows large scale motions at the solar surface based on the Hα emission. [NOAO/AURA/NSF]

The effect is the same as if the light had been passed through a curved slit. If we then use a prism or grating to spread out the different wavelengths, we will obtain a line spectrum, though each line will appear curved. This spectrum is called a *flash spectrum* because it is only visible for the brief instant that the Moon is covering all of the photosphere but not the chromosphere. Note that the spectrum shows emission lines. This is because there is no strong continuum to be absorbed.

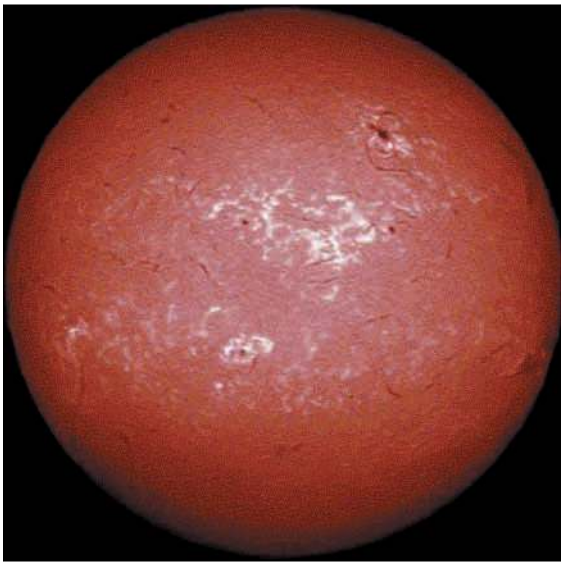

Fig 6.16. Hα image showing the chromosphere. [NASA]

When we study the spectra of the chromosphere we find that it is hotter than the photosphere. The chromospheric temperature is about 15 000 K. (The Sun doesn't appear this hot because the chromosphere is optically thin and doesn't contribute much to the total radiation we see.) We are faced with trying to explain how the temperature rises as we move farther from the center of the Sun. We will discuss this point in the next section, when we discuss the corona.

6.5 The corona

6.5.1 Parts of the corona

The corona is most apparent during total solar eclipses (Fig. 6.17), when the much brighter light

(a)

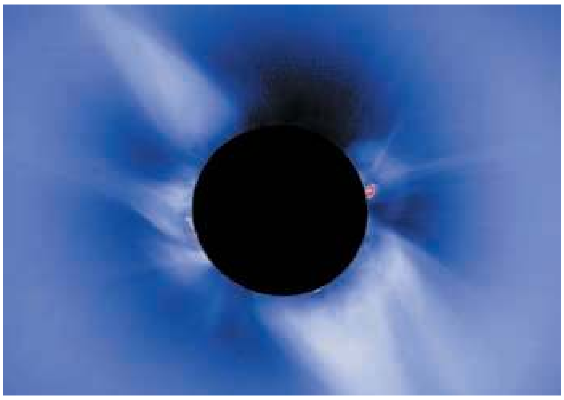

(b)

Fig 6.17. Two views of total solar eclipses, showing the corona. [(a) NOAO/AURA/NSF; (b) NASA] from the photosphere and chromosphere is blocked out. The corona is simply too faint to be seen when any photospheric light is present. You might think that we can simulate the effect of an eclipse by holding a disk over the Sun. If you try this, light that would come directly from the photosphere to your eye will be blocked out. However, some photospheric light that is originally headed in a direction other than directly at you will scatter off the atoms and molecules in the Earth's atmosphere, and reach you anyway (Fig. 6.18). This scattered light is only a small fraction of the total photospheric light, but it is still enough to overwhelm the faint corona. This is not a problem during solar eclipses, because the Moon is outside the atmosphere, so there is nothing to scatter light around it.

Therefore, solar eclipses still provide us with unique opportunities to study the corona. For this purpose, we are fortunate that the Moon subtends almost the same angle as the Sun, as viewed from the Earth. The Moon can exactly block the photosphere and chromosphere, but not the corona. Unfortunately, we do not have an eclipse of the Sun every month. We would if the Moon's orbit were in the same plane as the Earth's orbit around the Sun. However, the Moon's orbit is inclined by about 5°, so total eclipses of the Sun are rare events. The average time between total solar eclipses is about one and a half years. Even when one occurs, the total eclipse is observable from a band not more than 300 km wide, and totality lasts only a few minutes.

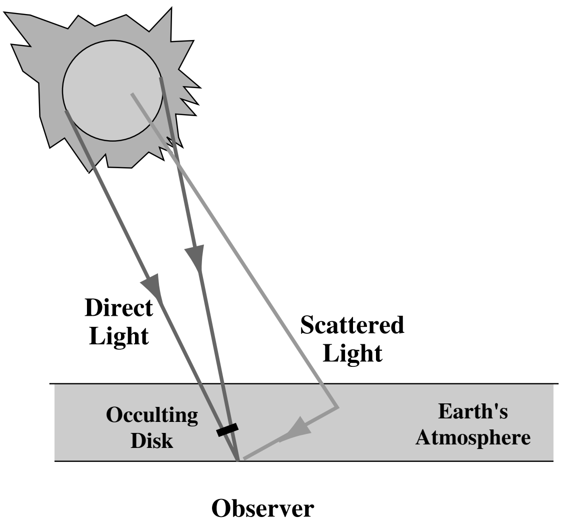

Fig 6.18. Effects of scattered light on corona studies. We can use an occulting disk, but sunlight can scatter off particles in the Earth's atmosphere and reach our telescope. Since the corona is very faint, and the Earth's atmosphere is very efficient at scattering, especially for blue light, this scattered light can overwhelm the direct light from the corona.

Solar astronomers take advantage of eclipses whenever possible, but also look for other ways to study the corona. It turns out that some ground-based non-eclipse observations are possible. Telescopes, called *coronagraphs*, have disks to block out the photospheric light, and reduce as much scattered light as possible. They are placed at high altitude sites, with very clear skies. For example, the Haleakala Crater on the island of Maui (operated by the University of Hawaii) is at an altitude of 3000 m (10 000 ft).

One way to get around the scattering in the Earth's atmosphere is to put a coronagraph in space. This is not quite as good as a solar eclipse, since space probes are not totally free of escaping gases. Some photospheric light is scattered by these gases. However, the results are much better than for a ground-based telescope. They also have an advantage over eclipse studies in that they allow for continuous study of the corona. For example, the Orbiting Solar Observatory 7 (OSO 7) provided observations of the corona for the period 1971–4.

There is an additional technique for studying the corona. It involves studying radio waves. Radio waves pass through the Earth's atmosphere and are not appreciably scattered. We therefore don't have to worry about the radio waves behaving like the visible light in Fig. 6.18.

In discussing what we have learned so far about the corona, we divide it into three parts:

(1) *The E-corona* is a source of emission lines directly from material in the corona. These lines come from highly ionized species, such as Fe XIV (13 times ionize iron). If we look at the Saha equation, discussed in Chapter 3, we see that highly ionized states are favored under conditions of high temperature and low density. The high temperature provides the energy necessary for the ionization.

The low density means that collisions leading to recombinations are rare.

(2) *The K-corona* (from the German *Kontinuierlich*, for continuous) is the result of photospheric light scattered from electrons in the corona.

(3) *The F-corona* (for Fraunhofer) is not really part of the Sun. It comes from photospheric light scattered by interplanetary dust. Since we are just seeing reflected photospheric light, the light still has the Fraunhofer spectrum. Both the F- and K-coronas appear at approximately the same angular distance from the center of the Sun, but there are experimental ways of separating their contributions to the light we see.

6.5.2 Temperature of the corona

When we analyze the abundance of highly ionized states, the Doppler broadening of lines and the strength of the radio emission, we find that the corona is very hot, about 2×10^6 K. As we have stated, the density is very low, approximately 10^{-9} times the density of the Earth's atmosphere.

Again, we must explain why a part of the atmosphere farther from the center of the Sun is hotter than a part closer to the center. We should note that it is not necessarily hard to keep something hot if it can't lose heat efficiently. For example, in a well insulated oven, once the required temperature has been reached, the heat source can be turned off and the temperature of the oven still stays high. An ionized gas (plasma) like the corona can lose energy only through collisions between the particles. For example, an electron and an ion could collide, with some of the kinetic energy going to excite the ion to a higher state. The ion can then emit a photon and return to its lower energy state. The emitted photon escapes and its energy is lost to the gas. If the lost energy is not replaced, the gas will cool.

Since collisions play an important role in the above process, the rate at which the gas can lose energy will depend on the rate at which collisions occur. The rate of collisions should be proportional to the product of the densities of the two colliding species. However, the density of each species is roughly proportional to the total gas density ρ (each being some fraction of the total). This means that the collision rate is proportional to ρ^2. Of course the amount of gas to be cooled is proportional to ρ. We can define a *cooling time* which is the ratio of the gas volume to be cooled (which is proportional to ρ) to the gas cooling rate (which is proportional to ρ^2). The cooling time is then proportional to $1/\rho$. Therefore, low density gases take longer to get rid of their stored heat.

Further, if the density is very low, a very high temperature doesn't necessarily mean a lot of stored energy. The energy is $(3/2)kT$ per particle. Even if the quantity kT is very large, if the total number of particles is very small, the energy stored is not as large as if the density were much higher.

Example 6.2 Energy density in the corona and the Earth's atmosphere

Compare the energy density (energy per unit volume) in the corona with that in the Earth's atmosphere.

SOLUTION

For each, the energy density is proportional to the density of particles n and the temperature T. (All other constants will drop out when we take the ratio.) Therefore

$$\frac{\text{energy density (corona)}}{\text{energy density (Earth)}} = \left[\frac{n(\text{corona})}{n(\text{Earth})}\right]\left[\frac{T(\text{corona})}{T(\text{Earth})}\right]$$

$$= [1 \times 10^{-9}]\left[\frac{2 \times 10^6}{3 \times 10^2}\right]$$

$$= 7 \times 10^{-6}$$

Even though the corona is so hot, its very low density gives it a lower energy density.

We must still come up with some explanation for getting energy into the corona. Some have suggested mechanisms in which oscillations near the surface of the Sun send supersonic sound waves (shock waves) into the Sun's upper atmosphere. In addition, there are mechanisms for heating that involve the Sun's magnetic field. These theories are still under study, and we still do not have a definitive picture of the energy balance in the corona.

When we study photographs of the corona, we find its structure is very irregular. We often see long streamers whose appearance varies with time. We think that these phenomena are related to the Sun's magnetic field, as are other aspects of solar activity (to be discussed in the following section).

6.6 Solar activity

6.6.1 Sunspots

When we look at photographs of the Sun (Figs. 6.1 and 6.19) we note a pattern of darker areas. As with the granulation, the dark areas are not really dark. They are just not as bright as the surrounding areas. The gas in these darker areas is probably at a temperature of about 3800 K. A closeup of these *sunspots* shows that they have a darker inner region, the *umbra*, surrounded by a lighter region, the *penumbra*.

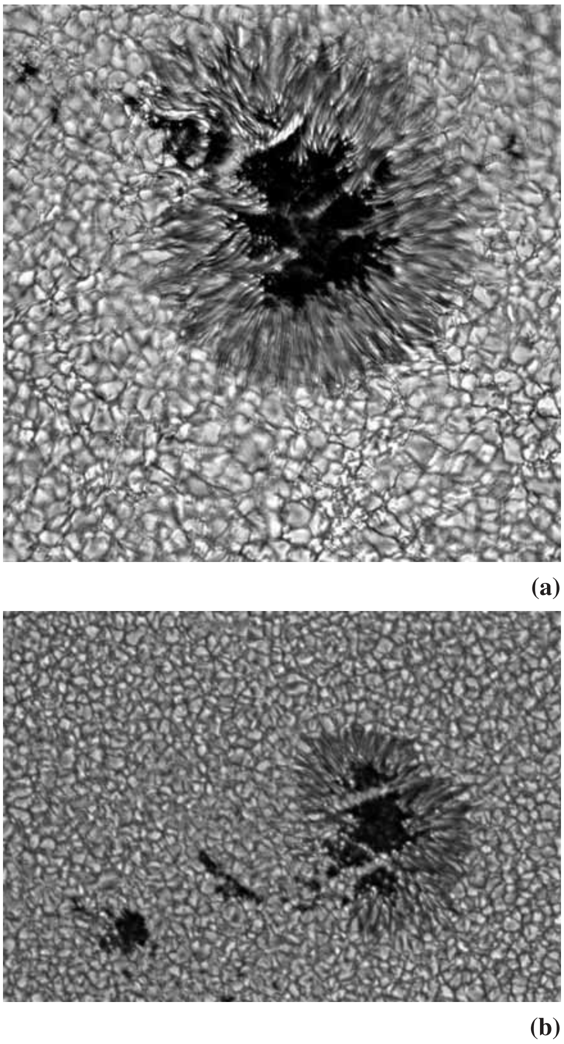

Fig 6.19. Sunspot images. The darker inner area of each spot is the umbra and the lighter outer area of each spot is the penumbra. The spots appear dark because the surrounding areas are brighter. [(a) NOAO/AURA/NSF; (b) NASA]

The number of sunspots on the Sun is not even approximately constant. It varies in a regular way, as shown in Fig. 6.20. It was realized in the mid-19th century that sunspot numbers follow an 11-year cycle. The number of sunspots in a peak year is not the same as in another peak year. However, the peaks are easily noticeable.

We see more regularity when we plot the height of each sunspot group above or below the Sun's equator as a function of when in the sunspot cycle they appear. This was done in 1904 by *E. Walter Maunder*. An example of such a diagram is shown in Fig. 6.21. Early in an 11-year cycle, sunspots appear far from the Sun's equator. Later in the cycle, they appear closer to the equator. This results in a butterfly-like pattern, and in fact these diagrams are sometimes called "butterfly diagrams".

When Maunder investigated records of past sunspot activity, he found that there was an extended period when no sunspots were observed. This period, from 1645 to 1715 is known as the *Maunder minimum*. This minimum has recently been reinvestigated by John A. Eddy, who found records to indicate that no aurorae were observed for many years during this period. Also during this time, weak coronae were reported during total solar eclipses. An unusual correlation was also found in the growth rings in trees, suggesting that altered solar activity had some effect on growth on Earth. The mechanism by which this takes place is poorly understood, but we can use the growth rings as an indicator of solar activity farther into the past than other records. A study of growth rings in old trees indicates that the Maunder minimum is not unique. There may have been several periods in the past with extended reduced solar activity.

Sunspots appear to be regions where the magnetic field is higher than on the rest of the Sun. In discussing sunspots, we should briefly review properties of magnetic fields and their interactions with matter. Magnetic fields arise from moving

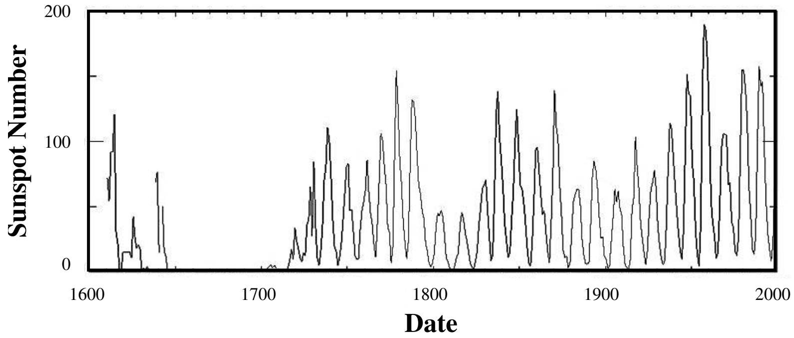

Fig 6.20. Numbers of sunspots per year as a function of year. The 11-year pattern is evident. Note that the number in a peak year is not the same from cycle to cycle. [NASA]

(including spinning) charges. Magnetic field lines form closed loops (Fig. 6.22). This is equivalent to saying that there are no point sources of magnetic charge, *magnetic monopoles*. (We will discuss the implications of the possible existence of magnetic monopoles in Chapter 21.) We call the closed loop pattern in Fig. 6.22 a *magnetic dipole*.

The magnetic field strength $\mathbf{B}$ is defined such that the magnetic force on a charge q, moving with velocity $\mathbf{v}$, is (in cgs units)

$$\mathbf{F} = q\,\mathbf{v} \times \mathbf{B}/c \tag{6.23}$$

where the **x** indicates a vector cross product. There is no magnetic force on a charge at rest, or on a charge moving parallel to the magnetic field lines. The force is maximum when the velocity is perpendicular to the magnetic field. The force is perpendicular to both the direction of motion and to the magnetic field, and its direction is given by the so-called "right hand rule". This means that the component of motion parallel to the field lines is not altered, but the component perpendicular to the field lines is. So, charged particles will move so that they spiral around magnetic field lines.

Through the forces that it exerts on moving charges, a magnetic field will exert a torque on a current loop. We can think of a current loop as having a magnetic dipole moment (as in Fig. 6.22), and the torque will cause the dipole to line up with the field lines. In this way, the dipole moment of a compass needle lines up with the Earth's magnetic field.

How do we measure the Sun's magnetic field? For certain atoms placed in a magnetic field, energy

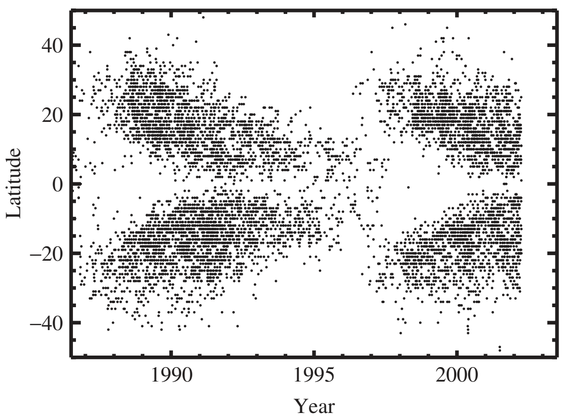

Fig 6.21. Butterfly diagram. This shows the distribution of sunspots in solar latitude as a function of time in the sunspot cycle. Early in a cycle, spots appear at higher latitudes; late in a cycle, they appear close to the equator. Note that a new cycle starts before the old cycle completely ends. [Roger Ulrich, UCLA, Mt Wilson. This study includes data from the synoptic program at the 150 ft Solar Tower of the Mt Wilson Observatory. The Mt Wilson 150 ft Solar Tower is operated by UCLA, with funding from NASA, ONR and NSF, under agreement with the Mt Wilson Institute]

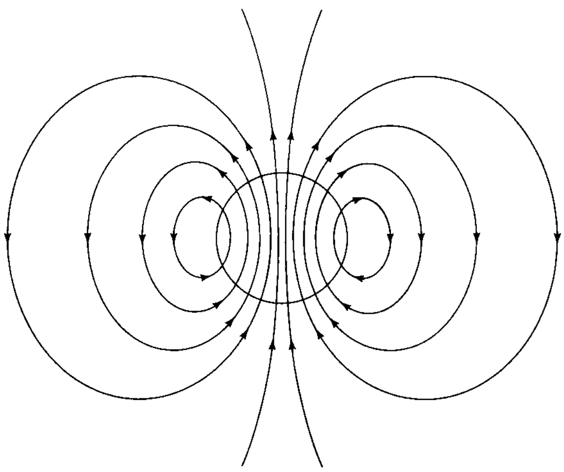

Fig 6.22. Field lines for a dipole magnetic field.

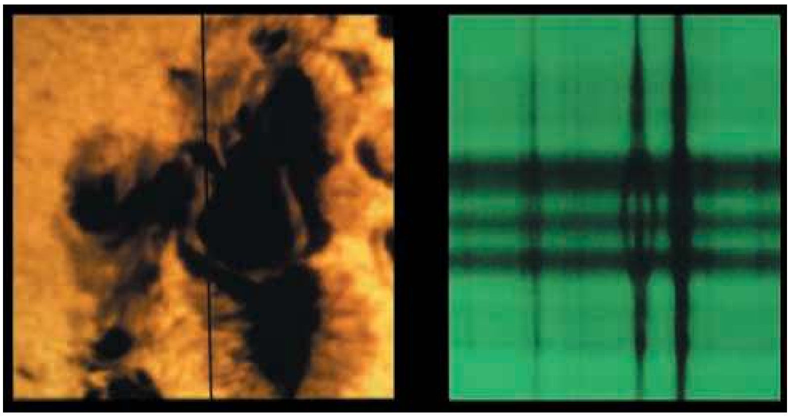

Fig 6.23. Zeeman effect in sunspots. (a) The placement of the spectrometer slit across a sunspot. (b) The spectrum at various positions along the slit. In the spectrum, away from the spot, the spectral lines are unsplit. In the center, near the spot, some of the spectral lines are split into three. The stronger the magnetic field the greater the splitting. [NOAO/AURA/NSF]

levels will shift. This is known as the *Zeeman effect* (Fig. 6.23). Different energy levels shift by different amounts. Some transitions that normally appear as one line split into a group of lines. The amount of splitting is proportional to the strength of the magnetic field. (We can check the amount of splitting in different atoms in various magnetic fields in the laboratory.) An image of the magnetic field strength over the whole Sun is shown in Fig. 6.24.

Measurements by *George Ellery Hale* in 1908 first showed that the magnetic fields are stronger in sunspots. He also found that sunspots occur in pairs, with one corresponding to the north pole of a magnet and the other to the south pole. In each sunspot pair, we can identify the one that "leads" as the sun rotates. In a given solar hemisphere, the polarity (i.e. N or S) of the leading spot of all pairs is the same. The polarity is different in the two hemispheres.

This polarity reverses in successive 11-year cycles. During one cycle all of the leading sunspots in the northern hemisphere will be magnetic north, while those in the south will be magnetic south. In the next cycle all the leading sunspots in the northern hemisphere will be magnetic south. The Sun's magnetic field reverses every 11 years! This means that the sunspot cycle is really a 22-year cycle in the Sun's magnetic field.

If the Sun's magnetic field arose in the core, as the Earth's does, we would expect it to be quite stable. (There is geological evidence that the Earth's magnetic field reverses periodically, but on geological time scales, not every 11 years.) We now think that the Sun's magnetic field arises below the surface, rather than in the core, as the Earth's does. We also know that the Sun does not rotate as a rigid body. By following sunspot groups (Figs. 6.25 and 6.26), we see that material at the equator takes less time to go around than material at higher latitudes. For example, it takes 25 days for

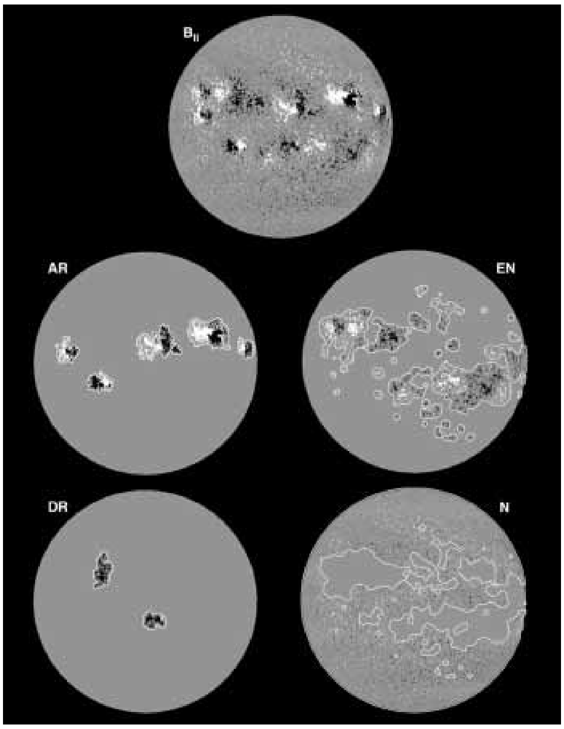

Fig 6.24. Solar magnetic field. This shows the result of observations of the Zeeman effect. Brighter areas correspond to stronger fields. [NOAO/AURA/NSF]

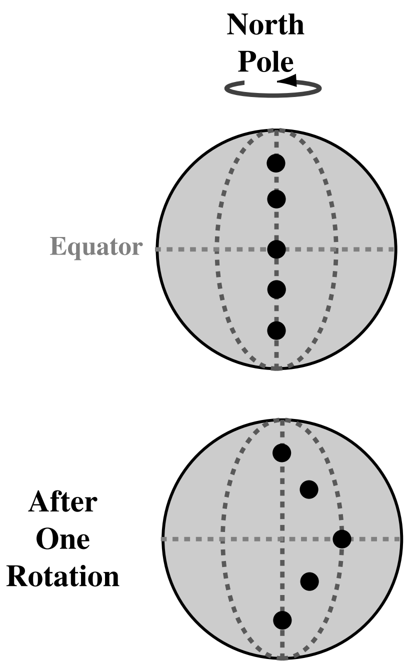

Fig 6.25. Differential rotation of the Sun, as traced out by sunspots. Since the Sun rotates faster at the equator than at higher latitudes, sunspots at the equator take less time to make one rotation than do those at higher latitudes. In this schematic diagram, a selection of sunspots starts at the same meridian, but, after one rotation of the Sun, they are on different meridians.

material at the equator to make one circuit, while it takes 28 days at 40° latitude.

As the Sun rotates differentially, the magnetic field lines become distorted. This is because the charged particles in the matter cannot move across field lines, so the field lines are carried along with the material. We say that the magnetic field is frozen into the material. The development of the magnetic field is shown in Fig. 6.27. As the field lines wind up, the field becomes very strong in places. Kinks in the field lines break through the surface. The sunspots apparently arise through some, as yet poorly understood, dynamo motion, involving convective motion and the magnetic fields.

6.6.2 Other activity

Sunspots are just one manifestation of solar activity related to the Sun's magnetic field. Another form of activity is the *solar flare*, shown in Fig. 6.28. A flare involves a large ejection of particles. Flares develop very quickly and last tens of minutes to a few hours. Temperatures in flares are high, up to 5×10^6 K. They also give off strong Hα emission, and flares are seen when the Sun is photographed through an Hα filter. Flares have been detected to give off energy in all parts of the

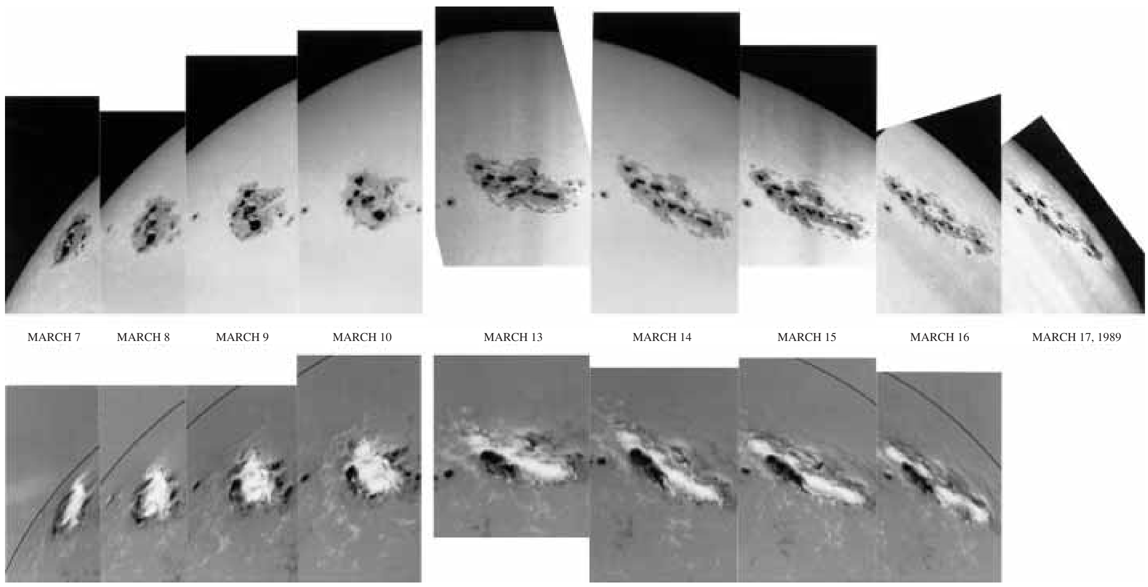

Fig 6.26. Differential rotation of the Sun, as traced out by sunspots. This sequence of images shows this effect on the Sun. [NOAO/AURA/NSF]

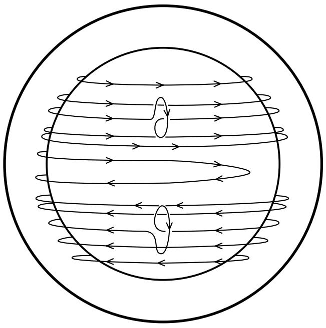

Fig 6.27. This shows how the solar magnetic field is twisted and kinked by the differential rotation of the Sun. It takes about 8 months for the field to wrap around once. The kinked parts of the field lines represent places where these loops come outside the Sun, allowing charged particles to follow those looped paths. [NASA]

electromagnetic spectrum. The cause of flares is not understood, but they appear to be related to strong magnetic fields and the flow of particles along field lines.

Solar activity is also manifested in *plages* (from the French word for "beach"). Plages are bright regions around sunspots. They show up in Hα images of the Sun. They remain after sunspots disappear. Plages are apparently chromospheric brightening caused by strong magnetic fields.

Filaments are dark bands near sunspot regions. They can be up to 10^5 km long. Filaments appear to be boundaries between regions of opposite magnetic polarity. When filaments are projected into space at the limb of the Sun, they appear as *prominences* (Fig. 6.29). Some prominences vary on short times scales while others evolve more slowly.

The *solar wind* is a stream of particles that are emitted from the Sun into interplanetary space. We can see the effects of the solar wind when we look at a comet that is passing near the Sun (Chapter 26). The tail of the comet always points away from the Sun. This is because the material in the tail is driven out of the head of the comet by the solar wind. The rate at which the Sun is losing mass is $10^{-14}\ M_{\odot}$/yr. The wind is still accelerating in its five- to ten-day trip from the Sun to Earth. At the Earth's orbit, the speed is about 400–450 km/s, and the density of particles is 5 to 10 cm^{-3}. The particles in the solar wind are positive ions and electrons. It is thought that the solar wind originates in lower density areas of the corona, called *coronal holes*.

The solar wind can have an effect on the Earth. Most of the solar wind particles directed at Earth never reach the surface of the Earth. The Earth's magnetic field serves as an effective shield, since the charged particles cannot travel across the field lines. Some of the particles, however, travel along the field lines and come closest to the Earth near the magnetic poles. These charged particles are responsible for the aurora displays. This explains why aurorae are seen primarily near the magnetic poles. When solar activity is increased, the aurorae become more widespread. The increased abundance of charged particles in our atmosphere also creates radio interference.

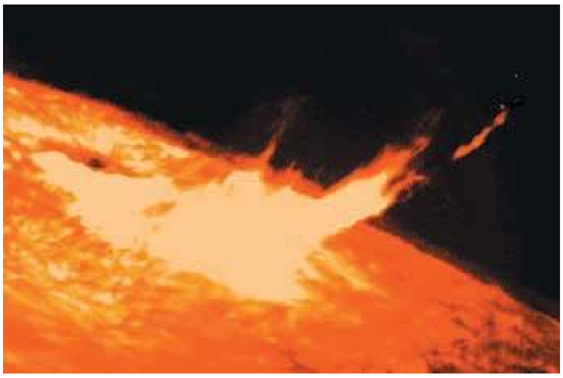

(a)

(b)

Fig 6.28. Images of solar flares. (a) Looking obliquely as the flare stands out from the surface. (b) In this photograph, taken through an Hα filter, we are looking down on a large solar flare from the side. This flare appears brighter than its surroundings in the Hα line. [NOAO/AURA/NSF]

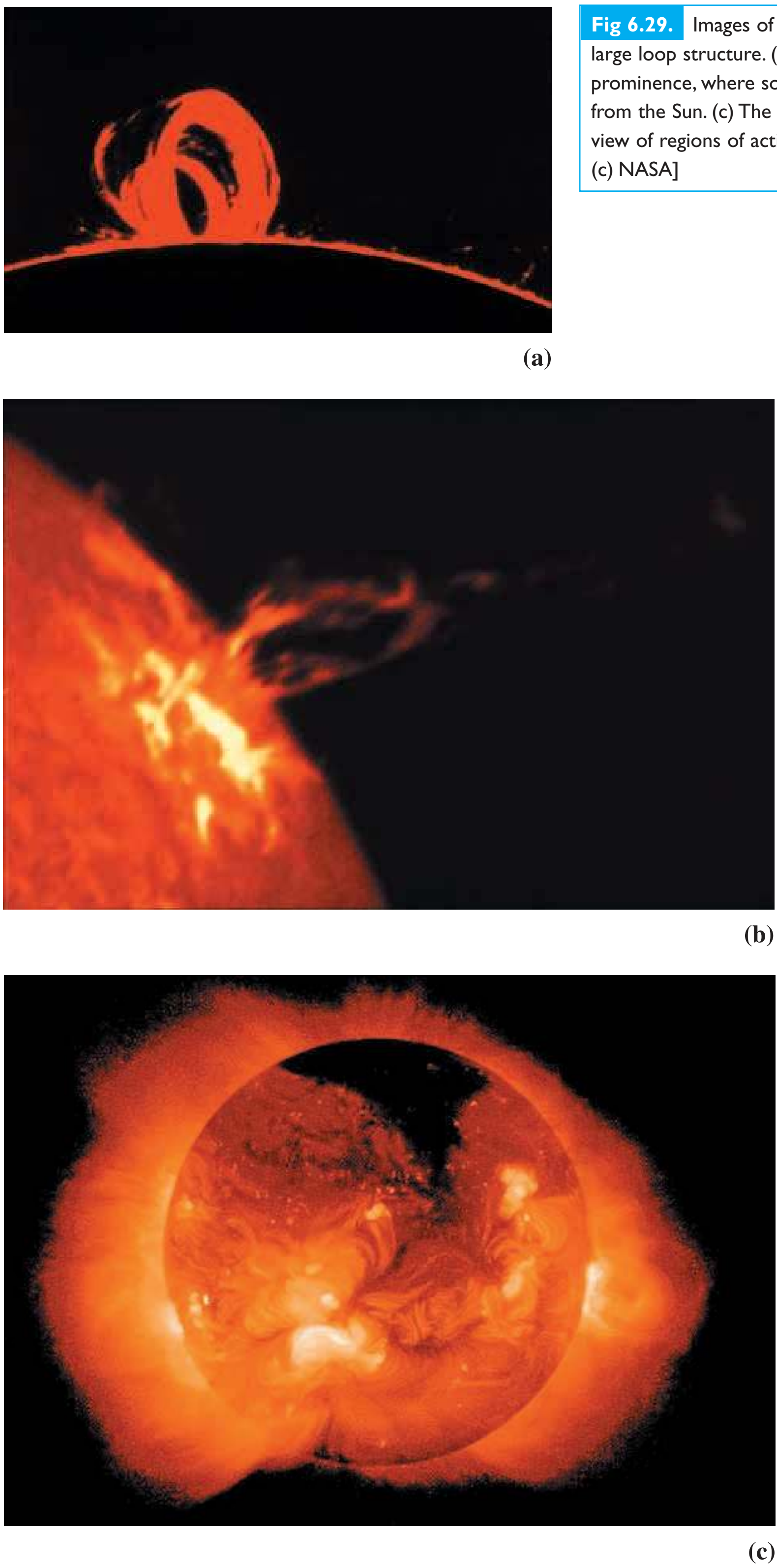

Fig 6.29. Images of large prominences. (a) This shows the large loop structure. (b) This Hα image shows an eruptive prominence, where some of the material may actually escape from the Sun. (c) The X-ray image of the Sun gives another view of regions of activity. [(a), (b) NOAO/AURA/NSF; (c) NASA]

Chapter summary

We looked in this chapter at the one star we can study in detail, the Sun.

Most of what we see in the Sun is a relatively thin layer, the photosphere. In studying radiative transfer, we saw how we can see to different depths in the photosphere by looking at different wavelengths. The distance we can see corresponds to about one optical depth.

The photosphere doesn't have a smooth appearance. Instead, it has a granular appearance, with the granular pattern changing on a time scale of several minutes. This suggests convection currents below the surface. Supergranulation suggests even deeper convection currents.

The chromosphere is difficult to study. In the chromosphere the temperature begins to increase as one moves farther from the center of the Sun. This trend continues dramatically into the corona. The best studies of the corona have come from total solar eclipses or from space.

We saw how sunspots appear in place of intensified magnetic fields, as evidenced by the Zeeman effect. The number of spots goes through a 22-year cycle, which includes a complete reversal in the Sun's magnetic field. The structure of the magnetic field is also related to other manifestations of solar activity, such as prominences.

Questions

6.1. In Fig. 6.3, what would be the effect on the total cross section of (a) doubling the density of particles, (b) doubling the length of the tube, (c) doubling the radius of each particle?

*6.2. (a) What does it mean to say that some sphere has a geometric cross section of 10^{-16} cm^2? (b) Suppose we do a quantum mechanical calculation and find that at some wavelength some atom has a cross section of 10^{-16} cm^2. What does that mean?

6.3. In studying radiative transfer effects, we let τ be a measure of where we are in a given sample, rather than position x. Explain why we can do this.

6.4. What does it mean when we say that something is optically thin?

6.5. Suppose we have a gas that has a large optical depth. We now double the amount of gas. How does that affect (a) the optical depth, (b) the amount of absorption?

6.6. Why do we need the "mean" in "mean free path"?

6.7. (a) Explain how we can use two different optical depth spectral lines to see different distances into the Sun. (b) Why is Hα particularly useful in studying the chromosphere?

6.8. What other situations have you encountered that have exponential fall-offs?

6.9. Explain how absorption and emission by the H^- ion can produce a continuum, rather than spectral lines?

6.10. Explain why we see a range of Doppler shifts over a spectral line.

6.11. How does Doppler broadening affect the separation between the centers of the Hα line and the Hβ line in a star?

6.12. What do granulation and supergranulation tell us about the Sun?

6.13. If the corona has $T = 2 \times 10^6$ K, why don't we see the Sun as a blackbody at this temperature?

6.14. Why can't you see the corona when you cover the Sun with your hand?

6.15. What advantages would a coronagraph on the Moon have over one on the Earth?

6.16. (a) Why does the F-corona still show the Fraunhofer spectrum? (b) Would you expect light from the Moon to show the Fraunhofer spectrum?

6.17. Why is the low density in the corona favorable for high levels of ionization?

6.18. (a) Why are collisions important in cooling a gas? (b) Why does the cooling rate depend on the square of the density? (c) How would you expect the heating rate to depend on the density?

6.19. Explain why charged particles drift parallel to magnetic field lines.

6.20. How are the various forms of solar activity related to the Sun's magnetic field?

Problems

6.1. Appendix G gives the composition of the Sun, measured by the fraction of the number of nuclei in the form of each element. Express the entries in this table as the fraction of the mass that is in each element. (Do this for the ten most abundant elements.)

6.2. Calculate the effective temperature of the Sun from the given solar luminosity, and radius, and compare your answer with the value given in the chapter.

6.3. Assume that for some process the cross section for absorption of a certain wavelength photon is 10^{-16} cm^2, and the density of H is 1 g/cm^3. (a) Suppose we have a cylinder that is 1 m long and has an end area of 1 cm^2. What is the total absorption cross section? How does this compare with the area of the end? (b) What is the absorption coefficient (per unit length)? (c) What is the mean free path? (d) How long a sample of material is needed to produce an optical depth of unity.

6.4. Suppose we have a uniform sphere (radius $R_\odot$) of 1 $M_\odot$ of hydrogen. What is the column density through the center of the sphere?

6.5. How large must the optical depth through a material be for the material to absorb: (a) 1% of the incident photons; (b) 10% of the incident photons; (c) 50% of the incident photons; (d) 99% of the incident photons?

6.6. If we have material that emits uniformly over its volume, what fraction of the photons that we see come from within one optical depth of the surface?

*6.7. Suppose we divide a material into N layers, each with optical depth $d\tau = \tau/N$, where τ is the total optical depth through the material and $d\tau \ll 1$. (a) Show that if radiation I_0 is incident on the material, the emergent radiation is

$$I = I_0\,(1 - d\tau)^N$$

(b) Show that this reduces to $I = I_0 e^{-\tau}$ (equation 6.19) in the limit of large N. (Hint: You may want to look at various representations of the function e^x.)

6.8. For what value of x does the error in the approximation $e^x \cong 1 + x$ reach 1%?

*6.9. Suppose we have a uniform sphere of radius R and absorption coefficient κ. We look along various paths, passing different distances p from the center of the sphere at their points of closest approach to the center. (a) Find an expression for the optical depth τ as a function of p. (b) Calculate $d\tau/dp$, the rate of change of τ with p. (c) Use your results to discuss the sharpness of the solar limb.

*6.10. Consider a charge Q near a neutral object. If the object is a conductor, charge can flow within it. The presence of the charge Q induces a dipole moment in the conductor, and there is a net force between the dipole and the charge. (a) Show that this force is attractive. (b) How does this apply to the possible existence of the H^- ion?

6.11. What is the thermal Doppler broadening of the Hα line in a star whose temperature is 20 000 K?

6.12. We observe the Hα line in a star to be broadened by 0.05 nm. What is the temperature of the star?

6.13. Compare the total thermal energy stored in the corona and photosphere.

6.14. (a) At what wavelength does the continuous spectrum from sunspots peak? (b) What is the ratio of intensities at 550 nm in a sunspot and in the normal photosphere? (c) What is the ratio of energy per second per surface area given off in a sunspot and in the normal photosphere?

6.15. How long does it take before material at the solar equator makes one more revolution than that at 40° latitude?

6.16. Calculate the energy per second given off in the solar wind?

*6.17. (a) What is the pressure exerted on the Earth by the solar wind? (Hint: Calculate the momentum per second on an object whose cross sectional area is that of the Earth.)
(b) How large a sail would you need to give an object with the mass of the space shuttle an acceleration of 0.1 g at the distance of the Earth from the Sun?

*6.18. To completely describe the radiative transfer problem, we must take emission into account as well as absorption. The *source function S* is defined so that $S\,d\tau$ is the increase in intensity due to emission in passing through a region of optical depth $d\tau$. This means that the radiative transfer equation should be written

$$dI/d\tau = -I + S$$

(a) If S is a constant, solve for I vs. τ, assuming an intensity I_0 enters the material. (b) Discuss your result in the limits $\tau \ll 1$ and $\tau \gg 1$.

Computer problems

6.1. Consider the situation in Fig. 6.4 with 1000 layers. Draw a graph of the fraction of the initial beam emerging from each layer, for total optical depths (a) 0.1, (b) 1.0, (c) 10.0. Show that the fraction emerging from the final layer agrees with equation (6.18).

6.2. Estimate the Doppler broadening for the Hα lines from the atmospheres at the mid-range of each spectral type (e.g. 05, B5, etc.). (Hint: Scale from the result in example (6.1).)